BJES Basrah Journal for Engineering Sciences

Basrah Journal for Engineering Sciences, Vol. 23, No. 2, 2023, 1-10

Original Article

Journal homepage: www.bjes.edu.iq
ISSN (Online): 23118385, ISSN (Print): 18146120

Study of the Vibration Characteristics of Rotating Shafts using Experimental and Finite Element Techniques

Luay M. Hassan[1,*] and Jaafar Khalaf Ali[2]

[1, 2] *Department of Mechanical Engineering, College of Engineering, University of Basrah, Basrah, Iraq*

Email: engpg.luay.majid@uobasrah.edu.iq, Jaafar.ali@uobasrah.edu.iq

Received: 1 September 2022; Revised: 6 October 2022; Accepted: 17 October 2022; Published: 30 December 2023

Abstract:– The rotor unbalances and misalignment in rotary machines are two major sources of vibration. rotor unbalance and misalignment is omnipresent in all rotating machinery widely used in many industrial applications, posing a serious threat to machine life and operation. The present work is an attempt to investigate the vibration characteristics (Amplitude, FFT, and time waveform) of a rotating mechanical system, which has an unbalanced rotor and misalignment. Vibration signals are acquired using an accelerometer mounted on the bearing housing nearer to the rotor. The FFT analysis of the acquired data revealed the response of an unbalanced rotor under operating conditions. Numerical analysis of the system using ANSYS portrayed the modal frequencies and mode shapes. Transient Structural analysis illustrates the response of the system to different mass unbalances. The results revealed that the magnitude of vibration characteristics significantly increases with excitation frequency and exciting force.

Keywords:– ANSYS, Flexible coupling, FFT analyzer, Unbalance, Vibration spectrum, Misalignment.

http://doi.org/10.33971/bjes.23.2.1

1. Introduction

Vibration analysis is performed to monitor the state of rotating machines under basic operating conditions, where developing problems must be identified before they reach critical stages and cause failure or sudden stop of machines, the design criteria for these machines depend on the weight and speed, the main concern in rotating machines is vibration and the resulting problems from these vibrations are many, including unbalance, misalignment, and cracks, so studying the dynamic properties is vital and important in designing systems mechanical rotary, When the rotor's inertia axis does not coincide with the geometric axis, unbalance is generated. Machine rotation produces a visible centrifugal force, which is generated by the rotor unbalance [1]. As a result of the shaft deflection and stress that results, the system's efficiency suffers, Vibration is a kind of transmission of rotational energy from rotating machines to their components. The system's unbalance serves as a visual representation of the process of transmission. Using the unbalanced response's vibration characteristics as a guide, vibration may be better regulated. Shaft and bearing dynamic stiffness have an impact on system reaction, as do rotor speed, geometric proportions, and mass distribution rotor system's dynamic vibration characteristics reflect the unbalance, which is represented in the unbalanced response's vibration, machine vibrations are a sign of problems and include important information on the nature and origin of the vibrations themselves. Model and signal-based techniques are used to identify the faults. using model-based techniques, defects' size and location may be identified. One of the most trustworthy ways to ascertain the dynamic properties of a system is via experimental inquiry since genuine features are shown as they are. Due to the inherent uncertainties in the boundary conditions and operational parameters, reliable modeling of systems with spinning components is a laborious task. Mode shapes that represent the system's dynamic behavior are discovered via further examination of the modal testing data. The approach that is most often used to identify the system's fundamental frequencies and mode shapes in the targeted frequency range is experimental modal analysis.

Rotating machinery used in several industrial applications is prone to a variety of mechanical problems. Misalignment is one of the most common mechanical problems. It is responsible for 60-70 % of all vibration-related machinery failures. Misalignment is problematic since it leads to the premature failure of couplings, bearings, seals, motor efficiency, etc. Inadvertent misalignment can lead to severe vibrations, which ultimately lead to the system's demise. Static and dynamic, multi-harmonic (i.e., 1X, 2X, 3X) system responses are caused by parallel misalignment alone [2].

Ahobal and Prasad (2019) [3] use comparison in measurements between the balanced condition of the mechanical system and the unbalanced state, the case was detected experimentally by transferring data and analyzing it with an FFT analyzer and comparing it with the theoretical results that were calculated by simulation using the ANSYS program. Findings showed that the excitation frequency has a substantial impact on the amplitude of vibration characteristics. The results show that the chosen operating range is devoid of critical speed.

Aboud and Ali (2021) [4] proposed a work that uses the effects of torsional, lateral, and longitudinal vibrations, on a ship's propulsion system are investigated. To investigate vibration at varying rotational speeds, a finite element model is set up. In this work, lateral and torsional vibrations are analyzed, modeled, and simulated with the help of MATLAB software. Additionally, ANSYS 2019 R3 is utilized in the investigation of specific marine propulsion system situations. where it was determined that the critical speed is inversely related to the change in diameter of the shaft, indicating that the diameter of propulsion shafts plays a key role and affects the extent of the reaction and resonant speed range. In addition to the bearing's response in a couple of unbalanced cases under varying stiffness, the amount of the vibration is inversely related to the stiffness, except in the case when the stiffness is 60 MN/m.

Ameen and Ali (2020) [5] Natural frequencies of a circular shaft have been determined using three EMA methods (i.e., impact roving accelerometer, impact roving hammer, and shaker roving accelerometer) in this study. An acceptable degree of error from the analytically predicted values is established for natural frequency. The five excitation techniques' mode shapes were graphed. The presence of similarity is proof in and of itself. In other words, the effectiveness of EMA has been shown. Each mode's damping ratio is measured experimentally. Produced findings that are within 2 % of the maximum percentage error of ANSYS's numerical values.

Jasim and Ali (2021) [6] used the non-contact vibration measurement method has been introduced by using a high-speed camera as a vibration measurement device. This method has all the advantages of the non-contact vibration measurements, other tests were accomplished by using the machinery faults simulator with two different fault cases, static unbalance, and couple unbalance. and by reading the information, the time domain, frequency domain, ODS, and phase differences, have been extracted for many points on the simulator rotor.

Khot and Khaire (2015) [7] studied the effect of misalignment with flexible flange connections with the help of an FFT analyzer to obtain the frequency spectrum using the experimental setup that was developed for their work. The study was done by experimental work distortion work (displacement by an amount of 1.5 mm). Between the two rotating shafts. Then simulate the rotary system using the ANSYS program within a specified speed range of (250 rpm to 1500 rpm). The vibration spectrum is gathered by modeling and testing with various stimulation frequencies, and it is observed that they are tightly connected. The results revealed that in second harmonics, or for parallel misalignment, the shaft should operate at 2X its normal speed, and for angular misalignment, at 1X its normal speed.

Jalan and Mohanty (2009) [8] presented a work in which, the resulting vibration was studied by the presence of two types of problems in the mechanical system prepared for this purpose (unbalance and misalignment). The theoretical part was based on a proposed system consisting of equations that were used in calculating the forces in the three directions (X, Y, Z) resulting from these faults, and the results were identical in both cases. The method may be useful for large systems such as turbine shafts, gearboxes, and the like. One of the objectives of this work is:

1. The vibration is measured by means of a sensor placed in several places determined by the examiner for the purpose of transmitting the vibration signal to a special analysis device for this signal.

2. knowing the frequencies resulting from the vibration and diagnosing the faults in the machine and after diagnosing the faults early before they occur, leads to obtaining a long service life, which leads to a good and stable production process.

2. Fault modeling

2.1. Mathematical modeling of unbalance

Rotor systems have a general motion equation, which looks like this [9]:

$$M\ddot{q} + C\dot{q} + \Omega G\dot{q} + Kq = 0 \tag{1}$$

or

$$M\ddot{q} + (C + \Omega G)\dot{q} + Kq = 0 \tag{2}$$

For calculation of Eigen values and Eigen vectors.

$$\begin{bmatrix} C+\Omega G & M \\ M & 0 \end{bmatrix} \frac{\mathrm{d}}{\mathrm{d}t} \begin{Bmatrix} q \\ \dot{q} \end{Bmatrix} + \begin{bmatrix} K & 0 \\ 0 & -M \end{bmatrix} \begin{Bmatrix} q \\ \dot{q} \end{Bmatrix} = \begin{Bmatrix} 0 \\ 0 \end{Bmatrix} \tag{3}$$

$$Ax + Bx = 0 \tag{4}$$

$$A = \begin{bmatrix} C+\Omega G & M \\ M & 0 \end{bmatrix}, \; B = \begin{bmatrix} K & 0 \\ 0 & -M \end{bmatrix}, \; x = \begin{Bmatrix} q \\ \dot{q} \end{Bmatrix} \tag{5}$$

where (M, C, G, *and* K) are matrices representing the mass, damping, gyroscopic, and stiffness of the rotor system, respectively. The node rotation and displacement terms are denoted by q.

Equation (6) is useful because it may be used to analyze and foretell the results of any potential unbalance. However, we believe that unbalance only occurs at the rotor's nodes, even though it can occur anywhere along the rotor's length. However, the manner in which the unbalance excites the modes within the frequency range of the machine is the crucial consideration, therefore this assumption is not as restricting as it may first appear. Therefore, unbalance at a specific group of nodes (in terms of the excitation delivered to a restricted group of modes) to unbalance over a wide area. This allows machines to be balanced by applying balance masses to a rotor in a limited number of planes.

$$M(\ddot{q} + \ddot{q_\varepsilon}) + \Omega G(\dot{q} + \dot{q_\varepsilon}) + C\dot{q} + K_q = 0 \tag{6}$$

$$M\ddot{q}+\Omega G\dot{q}+C\dot{q}+K_q=-M\ddot{q}_\varepsilon-\Omega G\dot{q}_\varepsilon \quad (7)$$

Because the excitation and response are harmonic.

$$\ddot{q}_\varepsilon=-\Omega^2 q_\varepsilon \quad (8)$$

$$M\ddot{q}+\Omega G\dot{q}+C\dot{q}+K_q=\Omega^2 Mq_\varepsilon-\Omega G\dot{q}_\varepsilon \quad (9)$$

2.2. Disk unbalance

One of the most common and significant causes of vibration in industrial rotor-bearing systems is rotor unbalance. When there is a disruption in the system's equilibrium, the system's dynamic behavior shifts. As a result of this shift [8].

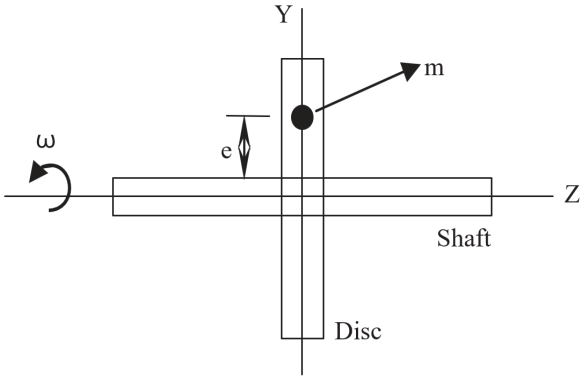

Fig. 1: Static disk unbalance.

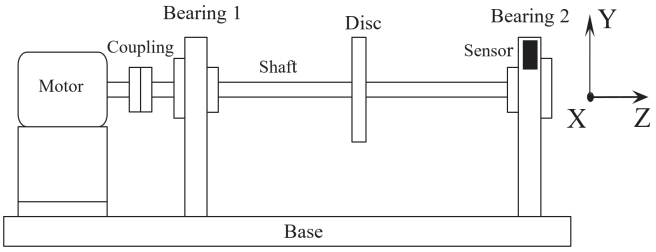

Fig. 2: Rotor–coupling–bearing test [8].

modeling the system. When the load is equivalent, the system's dynamics mimic the actual defective systems. The impact of both static and kinetic unbalances on the rotor system is modeled in the fault model for unbalance. Since the mass center of the mounted disk has moved, there is a static unbalance in the system that is comparable to a force. For the disk in the $x-y$ plane, the unbalanced forces act as [8].

$$F_x=me\omega^2\ \sin\omega t\ ,\ \ F_y=me\omega^2\ \cos\omega t \quad (10)$$

2.3. Coupling misalignment

Misalignment of the coupling in modern manufacturing, shaft misalignment in the rotor-bearing system is a typical and primary source of vibration in rotating machinery. In a system with misalignment, the parts are not coaxial because of their individual purposes. When two shafts aren't perfectly aligned, couplings are employed to make up the difference. Coupling is an often-overlooked yet crucial aspect of any rotor system, despite being relatively inexpensive in comparison to the whole. Complete line-outs may use either rigid or flexible couplings to join the individual shafts. In the case of stiff couplings, the link is modeled as the union of two beam elements. Flexible couplings are frequently employed in rotating machinery because they permit some misalignment between the axis of rotation of any two adjacent shafts [10].

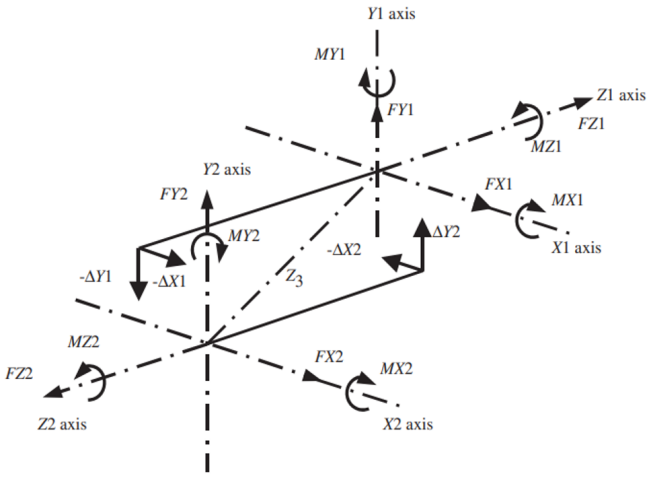

Fig. 3: Coupling coordinate system, parallel misalignment.

Parallel misalignment exerts on the machine's shaft are as follows [8]:

$$MX1=Tq\ \sin\theta_1+Kb\phi_1\ ,\ \ MX2=Tq\ \sin\theta_2-Kb\phi_2 \quad (11)$$

$$MY1=Tq\ \sin\phi_1-Kb\theta_1\ ,\ \ MY2=Tq\ \sin\phi_2-Kb\theta_2 \quad (12)$$

$$FX1=(-MY1-MY2)/Z3\ ,\ FX2=-FX1 \quad (13)$$

$$FY1=(MX1+MX2)/Z3\ ,\ FY2=FY2 \quad (14)$$

3. Experimental details

The device that is used to generate vibration signals for different types of faults is a Machinery Fault Simulator (MFS) shown in Fig. 4, which consists of a 1 HP and 60 Hz electric motor with an AC motor controller to control the speed of the motor, steel shaft of (3/4") diameter with a disc with the diameter (150 mm), mounted in the middle of the shaft that is used for applying loads and for unbalance faults simulation, two bearing holding the shaft and a coupling joint to connect the motor with the shaft. Connected one accelerometer type (BK 4370) of serial No. (776179) were mounted on the housing of the bearing, in the horizontal collect and monitor the raw vibration signals as shown in Fig. 5. The data acquisition (IDAC-6C) device is shown in Fig. 6, which is used to transfer the vibration signal from the accelerometer to a computer as vibration data for analysis. The main experimental part used in the generation of vibration signals in Fig. 4 are:

1. AC-motor controller
2. Tachometer
3. The Motor
4. Flexible coupling
5. Experimental bearing
6. Disc
7. Accelerometer

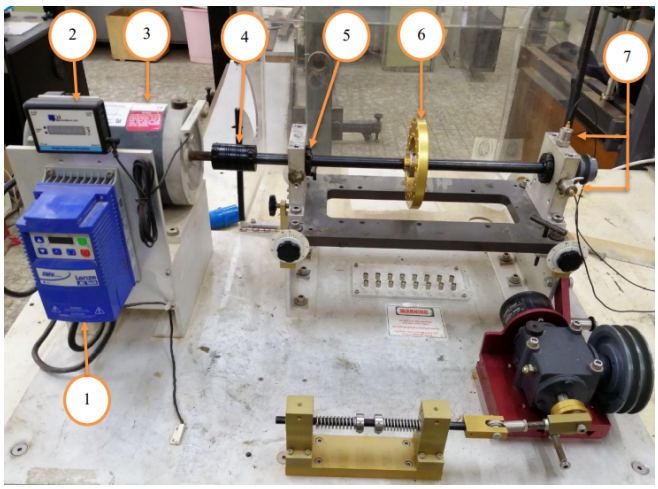

Fig. 4: Machinery fault simulator components.

Table 1: Operating conditions for the test.

Experimental parameter	Value	Unit
Rotary shaft diameter	19.05	mm
Rotary shaft length	59.6	cm
Mass unbalance additive to the disc	34.9	gm
Experiment speed	1500	rpm

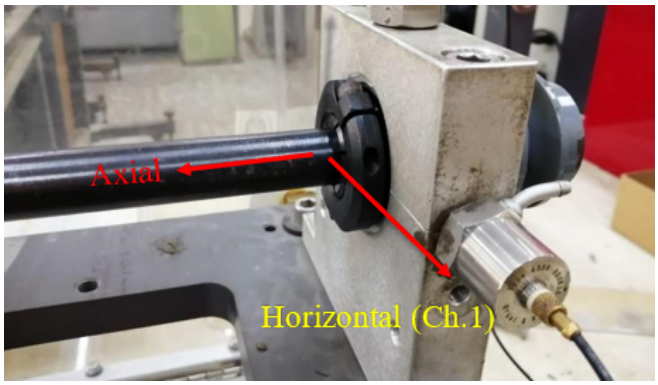

Fig. 5: Accelerometers.

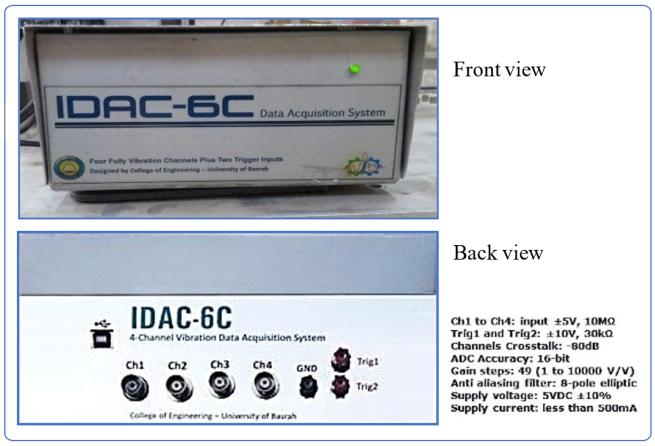

Fig. 6: Data acquisition (IDAC-6C).

3.1. Overview of the type of faults

3.1.1. Unbalance

The unbalance is the centrifugal forces that are generated from an excess mass or unequal distribution of masses with the centerline of rotation. Experimental unbalance is shown in Fig. 7.

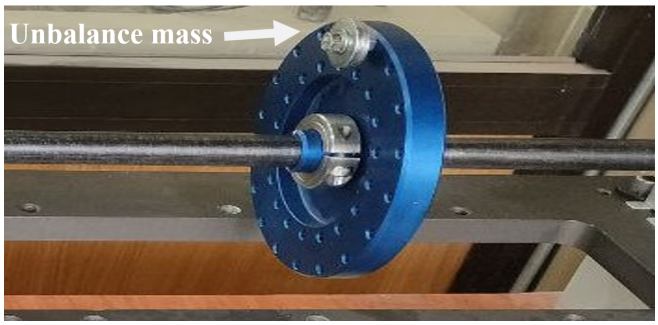

Fig. 7: the experimental unbalance.

$$F = mr\omega^2 \tag{15}$$

$$m = \pi r^2 \rho t \tag{16}$$

Where density (ρ) is 7850 kg/m^3. The radius is 6 cm when the frequency (ω) is 25 Hz (1500 rpm), the harmonic force generated is:

$$F = \pi \times 0.01^2 \times 0.016 \times 7850 \times 157^2 \times 0.06 = 58.418\ N \tag{17}$$

$$M_{the.} = \frac{F}{\omega^2 r} = \frac{58.418 \times 1000}{157^2 \times 0.06} = 39.5\ gram$$

$$Mr_{exp.} = Mr_{the.} \tag{18}$$

$$M_{exp.} = \frac{39.5 \times 60}{68} = 34.9\ gram \tag{19}$$

3.1.2. Misalignment

Misalignment is the vertical or angular offsetting in the centerline between the driving shaft and the driven machine. There are two types of misalignment depending on the type of offsetting, parallel and angular misalignment or combined. Fig. 8 shows the parallel misalignment if offset two sides of the Rotary shaft bracket. A four-pin type flexible flange coupling is used to connect the motor shaft.

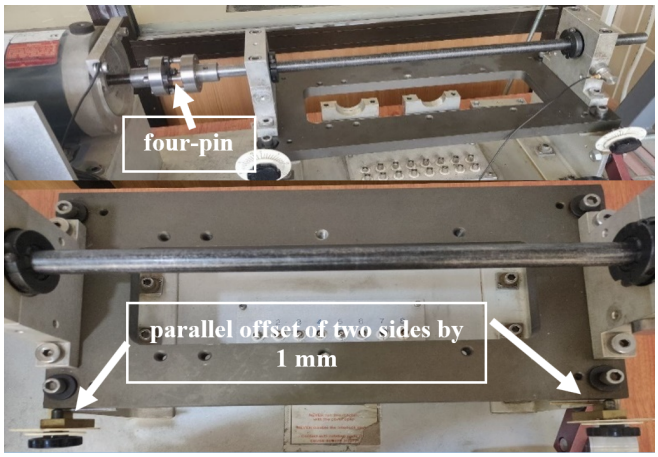

Fig. 8: the experimental parallel misalignment.

3.2. Experimental procedure

Initially, the accelerometer is attached to the bearing housing and connected to the FFT analyzer. An FFT analyzer and a computer are used to record the vibration data. Bearings are subjected to a typical vibration spectrum. Vibration frequency spectrum behavior was investigated at a speed of 1500 rpm in the experiment. The laboratory workflow diagram is shown in Fig. 9. A data acquisition device is used to collect the raw vibration signal generated by MFS at a speed value of 1500 rpm, and take new data for diagnosis [11].

The setting operation for the IDAC-6C software interface for the speed 1500 rpm are: For speeds 25 Hz (1500 rpm), the sample rate is 2048 sample/sec, the number of samples is 8192, the low-pass filter is 800 sample/sec and the high-pass filter is 0.3.

By MATLAB programming on the data that we obtained from the data acquisition device, it is possible to obtain vibration spectrum FFT with time waveform diagrams.

4. Finite element analysis of rotor bearing system

4.1. Modeling

Finite element analysis (FEA) is carried out on the shaft in the case under study using ANSYS (2020 R2) Workbench software, utilizing a built-in modal analysis tool. A transient Structural analysis module was selected for modeling. Geometry is drawn into SolidWorks 2021, then it is imported into the ANSYS module. To determine the modal frequencies, mode shapes, and steady-state response of the system operation under different unbalanced, conditions and

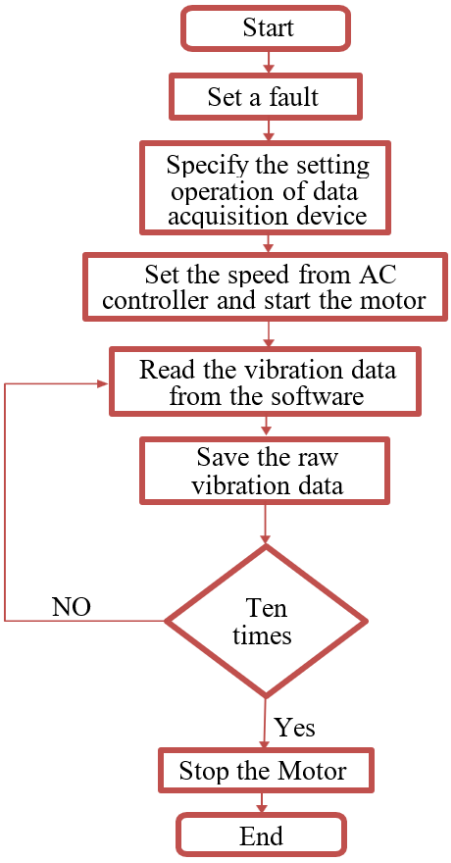

Fig. 9: Experimental Lap procedure.

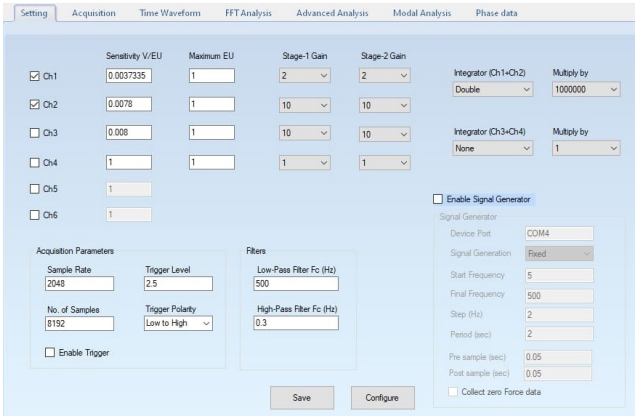

Fig. 10: setting operation for IDAC-6c software interface at speed 25 Hz (1500 rpm).

misalignment. In order to perform the FE analysis by ANSYS Workbench software, the following steps should be followed [12].

1. Problem description.
2. Building the geometry.
3. Define materials properties.
4. Mesh generation.
5. Apply loads and boundary conditions.

Fig. 11 shows the 3-D model created, with bearings specified in the FEA tool, for the numerical analysis of the system for both cases (unbalance with misalignment).

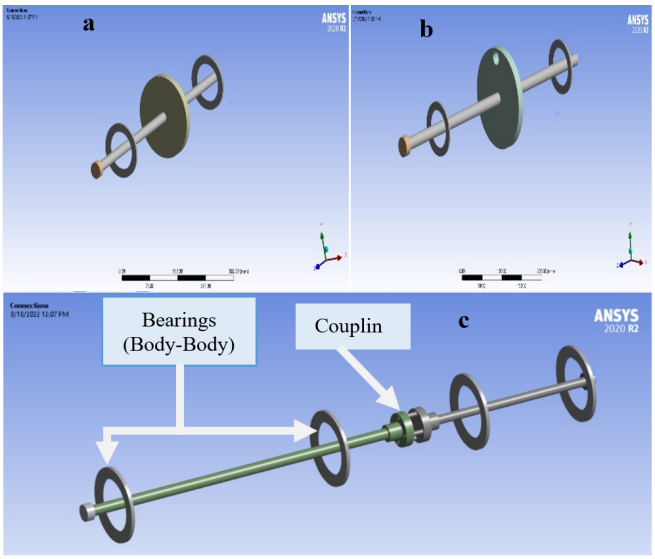

Fig. 11: 3-D numerical analysis model, (a) and (b) Unbalance case, (c) misalignment case.

Table 2: Material properties.

Material	Concrete	Aluminum alloy	Structural steel
Young's Modulus (MPa)	30000	71000	200000
Poison's ratio	0.18	0.33	0.3
Density (g/cm^3)	2.4	2.7	7.85

4.2. Meshing

Mapped meshing was selected for better accuracy, in this meshing time consumption is maximum as compared to free meshing. Mesh-by-face meshing for the rotating shaft and mesh-by-edge sizing for the disk (number of divisions = 40) as shown in Fig. 12.

4.3. Boundary condition and loading

The rotor shaft is supported by two identical pedestal bearings and a reason to select a pedestal bearing is that it should be fully supported on a flat, rigid surface to avoid distortion of the pedestal or deflection under load. The bearing (Body-Body) type is represented by choice from the connections list in the program ANSYS and the stiffness of the bearing is 5000 N/mm, and 1500 rpm was applied over the nodes of the shaft along the z-axis.

Case 1: Unbalance when a material of weight 39.5 gm is removed from the disk (disc defect).

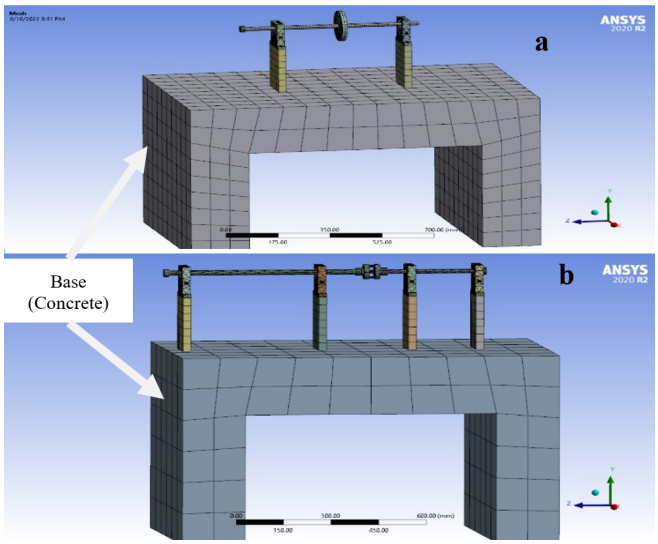

Fig. 12: Mesh of the rotor, (a) unbalance case, (b) misalignment case.

Table 3: Meshing of elements system.

Case	Mesh parameter	Description
Unbalance	Display style	Use geometry setting
	Solver preference	Mechanical APDL
	Element order	Program controlled
	Element size	Default
	Resolution	Default (2)
	Smoothing	High
	Number of element	4514
misalignment	Display style	Use geometry setting
	Solver preference	Mechanical APDL
	Element order	Program controlled
	Element size	Default (2)
	Resolution	1
	Smoothing	High
	Number of element	7617

- add rotational velocity by writing commands APDL in ANSYS. (ICROTATE, SPOOL1, OMEGA, $0,0,0,0,0,1,0,0,0,0$).
- speed: (1500 rpm or 25 Hz) was applied over the nodes of the shaft along the z-axis.
- Type of analysis in ANSYS: Transient Structural
- Number of Node:16595
- Hole diameter (mass removed) = 20 mm

Case 2: Parallel misalignment at bearing No. 1 and 2.

- Offset distance: (1 mm) in the direction of X (interval 0.0005).

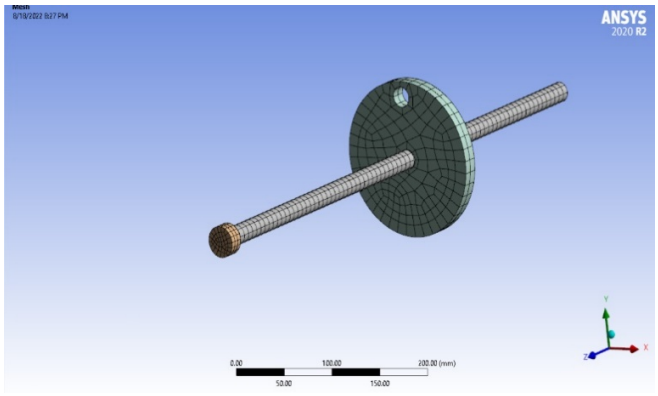

Fig. 13: meshed model of rotor bearing system (nodes 16595).

- add rotational velocity by writing commands APDL in ANSYS. (ICROTATE, SPOOL1, OMEGA, 0,0,0,0,0,1,0,0,0,0) (ICROTATE, SPOOL2, OMEGA, 1,0,0,1,0,1,0,0,0,0).
- speed: (1500 rpm) was applied over the nodes of the shaft along the z-axis. The horizontal movement of the shaft is constrained at one end of the shaft.
- Type of analysis in ANSYS: Transient structural.
- Number of Node: 17525

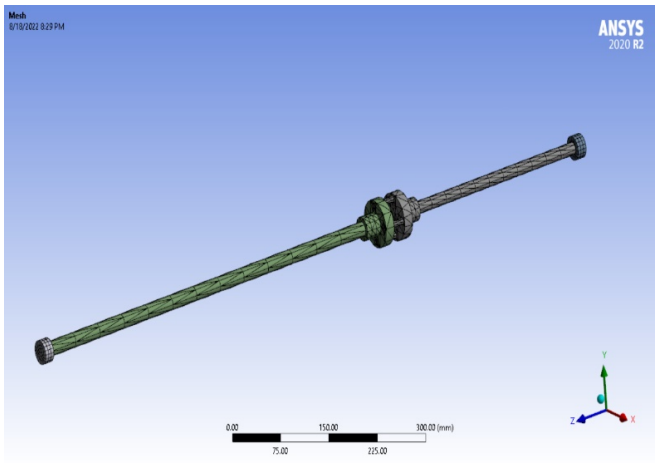

(a)

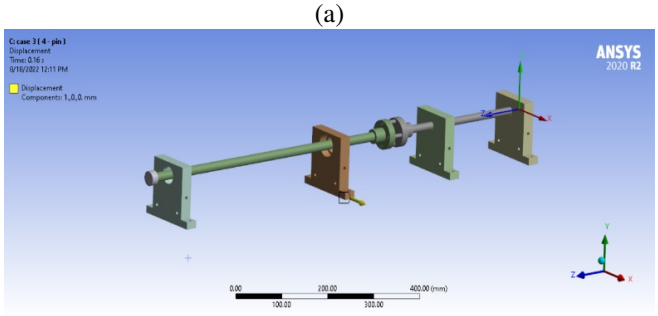

(b)

Fig. 14: (a) meshed model of rotor bearing system, (b) The direction of displacement of the support base of the rotating shaft.

Table 4: Execution time of cases in the program ANSYS.

Case	Execution time
Unbalance (in case of disc defect)	3 h 4 m
Parallel misalignment	1 h 58 m

5. Results and discussion

Case 1: Unbalance when a material of weight 39.5 gm is removed from the disk. Experimental and simulation study has been carried out to investigate the effect of the unbalance of a rotating shaft in the vibration spectrum. The results of the experimental study and simulation study for the baseline condition case and the unbalance are also compared.

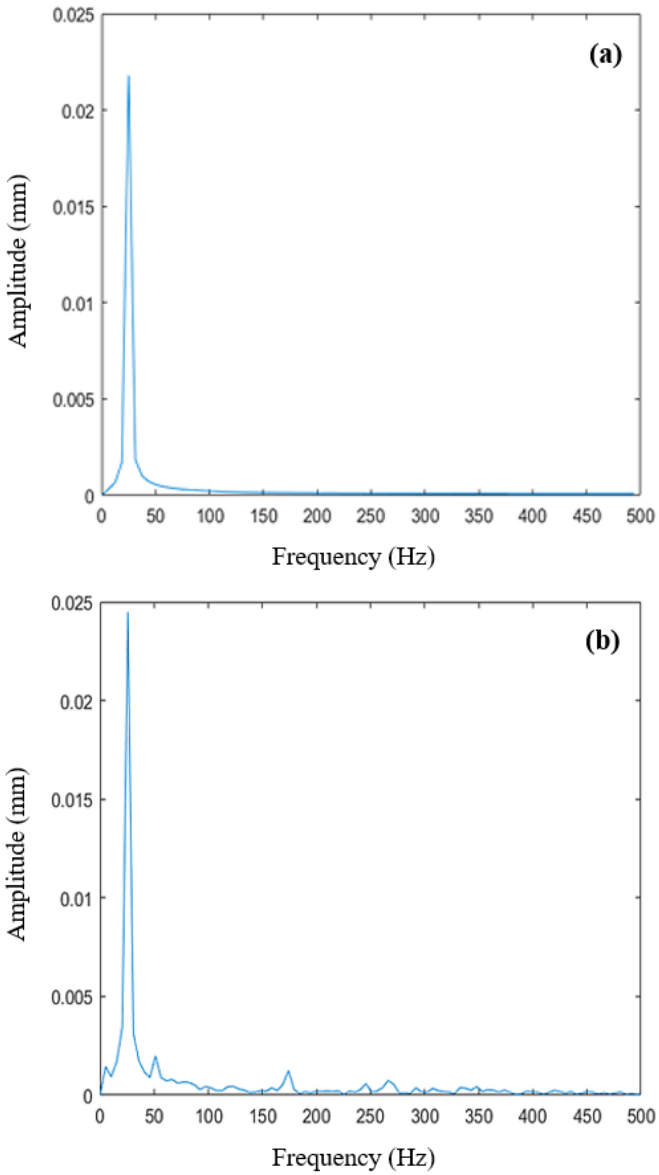

Fig. 15: Amplitude with frequency plot (for 1500 rpm), (a) simulation study, (b) Experimental study.

Fig. 15 shows the vibration spectrum acquired on the bearing away from the motor bearing 2(non-drive-end (NDE)) at a frequency (25 Hz) for operating conditions at

unbalancing. The results obtained from the experimental study and simulations, with a test speed of (1500 rpm) as shown. It was noticed that the maximum noticeable vibration amplitude was (0.02448 mm) for the experimental study, and its amount was (0.02179) for the simulation study. As it was noted from the above graph, the amplitudes are not identical in the results of the two studies. Note that the amplitude is high in the experimental study compared with the simulation study. However, there is close agreement between experimental and simulation results. From the above diagram, the dominant peak of the rotating shaft when unbalanced is 1X of the shaft speed.

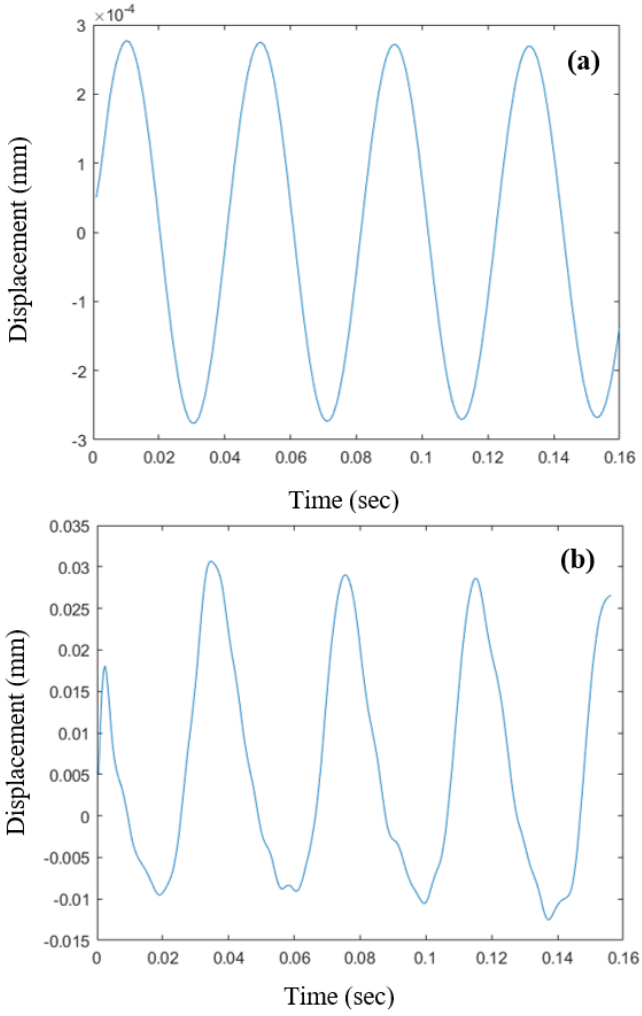

Fig. 16: Unbalance responses in the time domain, (a) 1500 rpm simulation study, (b) 1500 rpm experimental study.

When excitation frequency is increased, the magnitude of vibrational amplitudes increases, Fig. 16 shows the responses in the time domain for two studies (Experimental and simulation).

Case 2: Parallel misalignment Observed through the experiment and simulation, the vibration spectrum acquired experimentally and simulation on end bearing (non-drive-end (NDE)) at a frequency of 25 Hz, the maximum vibration amplitudes observed at 25 Hz are 0.011003 mm and 0.01187 mm by experimental and simulation respectively. This

Table 5: Overall amplitude in horizontal directions, non-drive-end (NDE) bearings of the rotor.

Speed	Amplitude (mm)		
	Bearing end	Simulation study	Experimental study
		Horizontal (H)	Horizontal (H)
1500 rpm 25 Hz	NDE	0.02179	0.02448

shows that the amplitude of vibration in the simulations is less than it is in the experiment. However, the simulation and experimental results are in close agreement regarding dominant frequency since the peak amplitude is seen at 50 Hz which is 2X of the shaft speed. As shown in Fig. 17.

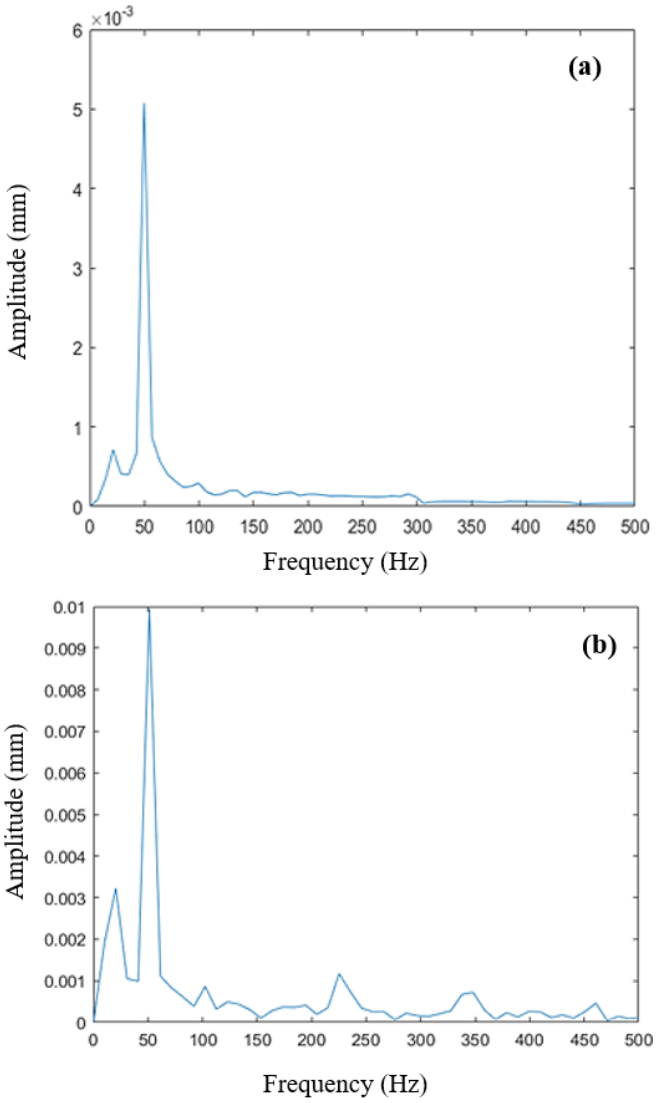

Fig. 17: Amplitude with frequency plot (1500 rpm), (a) simulation study, (b) experimental study.

When excitation frequency is increased, the magnitude of vibrational amplitudes increases, Fig. 18 shows the responses in the time domain for two studies (Experimental and Simulation).

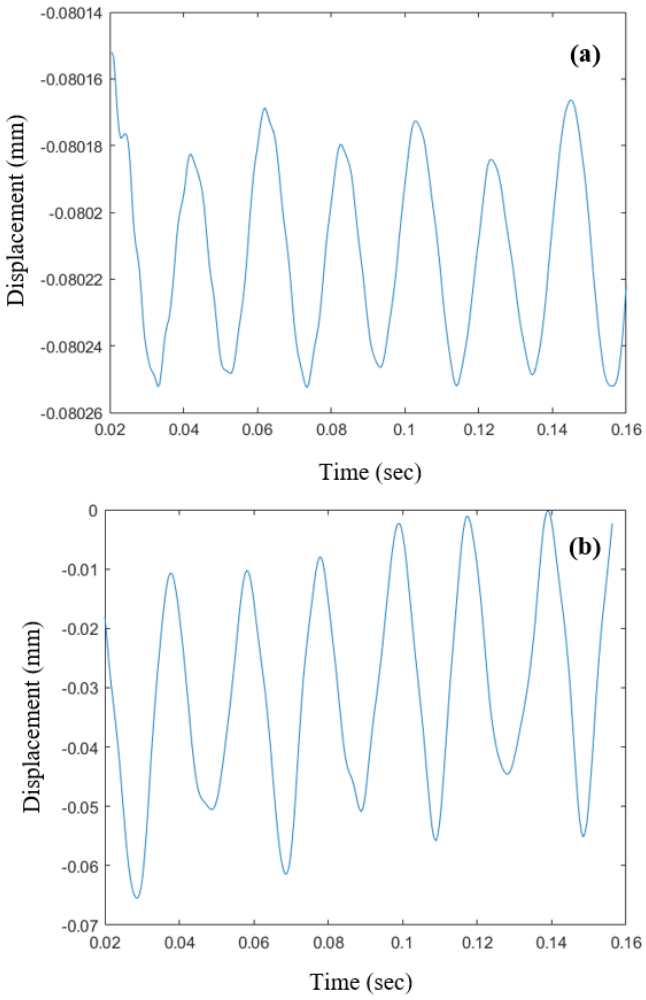

Fig. 18: Parallel misalignment responses in the time domain at 1500 rpm, (a) Simulation study, (b) Experimental study.

Table 6: Overall amplitude in horizontal directions, non-drive-end (NDE) bearings of the rotor.

Speed	Amplitude (mm)		
	Bearing end	Simulation study	Experimental study
		Horizontal (H)	Horizontal (H)
1500 rpm 25 Hz	NDE	0.00507	0.00993

6. Conclusions

For the unbalanced case, the following conclusions can be obtained as a result of the experimental analysis and the theoretical analysis that was used to verify the operating conditions of the vibration characteristics of the rotating mechanical system.

The FFT diagrams indicate the harmonics of the vibration characteristics that are moving toward the peak value and show the presence of the first typical frequency.

For the misalignment case, the vibration spectra are obtained through experimental and simulation for various excitation frequencies and found to be in close agreement. Results from both the experimental and simulated studies showed that the second harmonics (2X), or twice the shaft running speed in the case of parallel misalignment, best characterize the misalignment. In contrast, the amplitude of vibration was much lower in the case of an aligned system. In addition, it can be seen that the amplitude of vibration grows in tandem with the excitation frequency.

Nomenclature		
Symbol	Description	SI Units
$B, K4370$	Accelerometer	-
E	Elastic modulus	Pa
EMA	Experimental Model Analysis	-
F	Unbalance Force	N
FFT	Fast Fourier Transform	-
$IDAC-6C$	Data acquisition	-
K	Bearing stiffness	N/mm
M	Unbalance Mass	kg
M_{exp}	Experimental mass unbalance	kg
M_{the}	Theoretical mass unbalance	kg
MFS	Machinery Fault Simulator	-
ODS	Operation Deflection Shape	-
r	The distance from the center of mass of the unbalance from the center of rotation	mm
RMS	Root Mean Square	-
rpm	Revolutions Per Minute	rad
t	Disc thickness	mm
Greek Symbols		
Symbol	Description	SI Units
ρ	Density	kg/m^3
ω	Frequency	rad/sec

References

[1] R. Tamrakar and N. Mittal, "Comparison of response to unbalance of overhung rotor system for different supports," *Int. J. Mech. Eng. Technol*, vol. 8, no. 3, pp. 56–65, 2017.

[2] D. P. Hujare and M. G. Karnik, "Vibration responses of parallel misalignment in al shaft rotor bearing system with rigid coupling," *Materials Today: Proceedings*, vol. 5, no. 11, pp. 23 863–23 871, 2018.

[3] N. Ahobal *et al.*, "Study of vibration characteristics of unbalanced overhanging rotor," in *IOP Conference Series: Materials Science and Engineering*, vol. 577, no. 1. IOP Publishing, 2019, p. 012140.

[4] A. A. H. Aboud and J. K. Ali, "Study of effective parameters in stability and vibration of marine propulsion shafting systems," in *Journal of Physics: Conference Series*, vol. 1973, no. 1. IOP Publishing, 2021, p. 012032.

[5] Y. M. Ameen and J. K. Ali, "Theoretical and experimental modal analysis of circular cross-section shaft," in *IOP Conference Series: Materials Science and Engineering*, vol. 745, no. 1. IOP Publishing, 2020, p. 012066.

[6] H. S. Jasim and J. K. Ali, "Detecting vibration problems in machines and structures using motion capturing by camera," *Basrah Journal for Engineering Sciences*, vol. 21, no. 1, 2021.

[7] S. Khot and P. Khaire, "Simulation and experimental study for diagnosis of misalignment effect in rotating system," *Journal of Vibration Analysis, Measurement, and Control*, vol. 3, no. 2, pp. 165–17, 2015.

[8] A. K. Jalan and A. Mohanty, "Model based fault diagnosis of a rotor–bearing system for misalignment and unbalance under steady-state condition," *Journal of sound and vibration*, vol. 327, no. 3-5, pp. 604–622, 2009.

[9] M. I. Friswell, *Dynamics of rotating machines*. Cambridge University Press, 2010.

[10] S. D. Dere and L. Dhamande, "Rotor bearing system fea analysis for misalignment," 2017.

[11] A. Abdulrazzaq and J. K. Ali, "Surveys for artificial immune recognition system and comparison with artificial neural networks and support vector machines in intelligent fault diagnosis of rotating machines," *Int. J. Mech. Eng. Technol.*, vol. 10, no. 1, pp. 1686–1709, 2019.

[12] Y. M. Ameen and J. K. Ali, "Flexible rotor balancing without trial runs using experimentally tuned fe based rotor model," *Basrah Journal for Engineering Sciences*, vol. 21, no. 1, 2021.